



# Carbon dioxide uptake overrides methane emission at the air-water interface of algae-shellfish mariculture ponds: Evidence from eddy covariance observations



Yiping Zhang<sup>a</sup>, Zhangcai Qin<sup>b,c</sup>, Tingting Li<sup>c,d</sup>, Xudong Zhu<sup>a,c,\*</sup>

<sup>a</sup> State Key Laboratory of Marine Environment Science, Key Laboratory of the Coastal and Wetland Ecosystems (Ministry of Education), Coastal and Ocean Management Institute, College of the Environment and Ecology, Xiamen University, Xiamen, Fujian 361102, China

<sup>b</sup> School of Atmospheric Sciences, Guangdong Province Key Laboratory for Climate Change and Natural Disaster Studies, Sun Yat-sen University, Zhuhai, Guangdong 519000, China

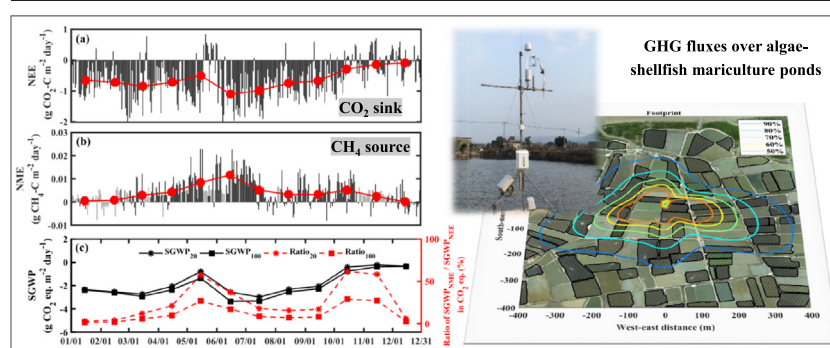
<sup>c</sup> Southern Marine Science and Engineering Guangdong Laboratory (Zhuhai), Zhuhai, Guangdong 519000, China

<sup>d</sup> LAPC, Institute of Atmospheric Physics, Chinese Academy of Sciences, Beijing 100029, China

## HIGHLIGHTS

- Mariculture ponds are biogeochemical hotspots of greenhouse gas (GHG) cycling
- Net GHG fluxes between mariculture ponds and the atmosphere are not well understood
- First year-round measurements of CO<sub>2</sub> and CH<sub>4</sub> fluxes via eddy covariance method
- Climate benefits of algae-shellfish mariculture ponds are dominated by CO<sub>2</sub> sink

## GRAPHICAL ABSTRACT



## ARTICLE INFO

### Article history:

Received 20 October 2021

Received in revised form 26 December 2021

Accepted 29 December 2021

Available online 4 January 2022

Editor: Pingqing Fu

### Keywords:

Greenhouse gas

Methane

Global warming potential

Razor clam

## ABSTRACT

Mariculture ponds are widely distributed along the coastal regions and have been increasingly recognized as biogeochemical hotspots of air-water greenhouse gas (GHG) fluxes, but their source/sink dynamics and climate benefits have not been well understood. Due to strong temporal variations of GHG fluxes over mariculture ponds, previous studies based on short-term or discrete flux measurements have large uncertainty in assessing GHG budgets and their radiative effects. In this study, we examined the temporal variations of air-water GHG fluxes, net CO<sub>2</sub> exchange (NEE) and net CH<sub>4</sub> exchange (NME), and their environmental controls, based on one-year (2020) continuous eddy covariance (EC) measurements over algae-shellfish mariculture ponds (razor clam) in a subtropical estuary of Southeast China. The results showed that (a) annually the ponds acted as a strong CO<sub>2</sub> sink of  $-227.7 \text{ g CO}_2\text{-C m}^{-2}$  and a weak CH<sub>4</sub> source of  $1.44 \text{ g CH}_4\text{-C m}^{-2}$ , and thus the NME-induced warming effect offset 25.9% (12.1%) of the NEE-induced cooling effect at a 20-year (100-year) time horizon using the metric of sustained-flux global warming potential; (b) two GHG fluxes showed different diurnal and seasonal variations but both had stronger source/sink capacity in summer and more fluctuating fluxes in winter; (c) temporal variations of NEE and NME tended to be more regulated by photosynthetically active radiation and tidal salinity, respectively, but both of them were affected by water temperature and area proportion of algae ponds within the EC footprint. This is the first study to disentangle temporal variations of air-water GHG

\* Corresponding author at: State Key Laboratory of Marine Environment Science, Key Laboratory of the Coastal and Wetland Ecosystems (Ministry of Education), Coastal and Ocean Management Institute, College of the Environment and Ecology, Xiamen University, Xiamen, Fujian 361102, China

E-mail address: [xdzhu@xmu.edu.cn](mailto:xdzhu@xmu.edu.cn) (X. Zhu).

fluxes over mariculture ponds based on simultaneous EC measurements of CO<sub>2</sub> and CH<sub>4</sub> fluxes. This study highlights the climate benefits of algae-shellfish mariculture ponds as biogeochemical hotspots by exerting a net radiative cooling effect dominated by the CO<sub>2</sub> sink.

## 1. Introduction

Atmospheric carbon dioxide (CO<sub>2</sub>) and methane (CH<sub>4</sub>) have attracted increasing attention since they are the two most important anthropogenic greenhouse gases (GHG) contributing >80% of global warming (IPCC, 2021). As a hotspot of GHG fluxes, aquatic ecosystems have been recognized as an important component of regional and global carbon cycles (Raymond et al., 2013; Gao et al., 2020). In comparison with GHG flux studies on large aquatic ecosystems like rivers, lakes, and reservoirs (Gerardo-Nieto et al., 2017; Woszczyk and Schubert, 2021), there are relatively fewer studies on aquaculture ponds that are smaller but widely distributed (Yang et al., 2020a). Recent studies have found small aquaculture ponds are important carbon sources (Wu et al., 2018; Yang et al., 2018b; Yuan et al., 2019; Yuan et al., 2021); however, most of these findings are based on GHG flux measurements within freshwater systems. Current GHG flux studies on mariculture systems like shrimp and shellfish ponds are still very limited, although mariculture ponds are widely distributed along the coasts such as China, occupying the largest area ( $1.9 \times 10^6$  hm<sup>2</sup>) and production ( $2.1 \times 10^7$  t) around the world (Fisheries Department of Agriculture Ministry of China, 2021).

The GHG fluxes across the water-air interface of mariculture ponds are influenced by environmental controls and human management. On the one hand, a variety of physical, chemical, and biological factors related to biogeochemical cycles can regulate GHG fluxes in mariculture ponds (Holgerson, 2015). On the other hand, intensive human management like feeding, water exchange, and aeration, can also significantly affect the GHG exchange (Chen et al., 2016a; Yuan et al., 2019). As a result of the combined effects from these regulating factors, the GHG fluxes over mariculture ponds have strong temporal variations and spatial heterogeneity. Some studies have assessed GHG fluxes and their warming potentials in mariculture ponds (Chen et al., 2016a; Yang et al., 2019a; Zhang et al., 2020b), but their assessments could have large uncertainty since few of them acquired GHG flux measurements in a long-term and continuous manner.

First, previous studies showed obvious diurnal and seasonal variations in GHG fluxes of mariculture ponds (Aime et al., 2018; Hu et al., 2020a; Zhang et al., 2020b). For example, most field measurements were conducted during daytime or over a few discontinuous days, and thus the flux measurements could bias since short-term or discontinuous measurements failed to capture the large temporal variations in GHG fluxes (Yang et al., 2013; Wilson et al., 2015). Second, although studies had compared GHG fluxes among ponds with different farming types or various functional areas within a pond (Yang et al., 2019b), these comparisons could suffer from insufficient spatial representation since they often focused on only a few ponds. Third, most studies estimated GHG fluxes using floating chamber-based methods; these methods could suffer from systematic errors since in principle they did not cover all flux transport pathways across the water-air interface. For example, CH<sub>4</sub> emissions were transported through ebullition (Yang et al., 2020b) in addition to diffusion and plant-mediated pathways, and thus chamber-based measurements could underestimate the emissions without covering ebullition-related efflux. Fourth, mariculture ponds had various farming activities with different farming species and management, both of which might heavily affect the magnitude of GHG fluxes in mariculture ponds (Yuan et al., 2019). Previous GHG studies on aquaculture ponds mainly explored GHG fluxes associated with single-type farming activities such as fish, shrimp, and crab (Yang et al., 2017; Ma et al., 2018), few studies focused on shellfish farming activities, which might have significantly different GHG flux patterns due to intensive algae cultivation (Ren, 2021). Fifth, different GHG fluxes in mariculture ponds, like CO<sub>2</sub> and CH<sub>4</sub> fluxes, were regulated by various biotic and

abiotic processes and thus often showed different temporal patterns, probably leading to strong temporal variations in global warming potential (GWP). Few studies had simultaneous and continuous measurements of different GHG fluxes over mariculture ponds, and the estimation of GWP based on short-term or discrete observations might not reflect the actual situation.

In summary, the uncertainty of estimated GHG fluxes in mariculture ponds is associated with high spatial and temporal heterogeneity, imperfect sampling and measuring methods, diversified farming species and management modes. This knowledge gap highlights the necessity of acquiring long-term and continuous GHG flux measurements. In this regard, the eddy covariance (EC) flux measurements can serve as a good option since EC is an automatic, non-destructive, and direct measuring technique having the capacity of capturing strong temporal variations of GHG fluxes. The EC approach has been widely used in various ecosystems including coastal wetlands (Lu et al., 2017; Erkkila et al., 2018; Zhao et al., 2019; Baldocchi, 2020); however, very few EC studies on GHG fluxes were applied in mariculture ponds.

To the best of our knowledge, there has been no such study focusing on assessing spatio-temporal dynamics of multiple GHG fluxes over mariculture ponds based on long-term high-frequency measurements of net ecosystem CO<sub>2</sub> (NEE) and CH<sub>4</sub> (NME) fluxes. The application of the EC approach can help close this knowledge gap. In this study, we examine one-year continuous EC measurements of NEE and NME over algae-shellfish mariculture ponds in a subtropical estuary of Southeast China. The specific objectives are (1) to analyze the temporal variations of NEE and NME across diurnal, daily, and seasonal time scales; (2) to examine the roles of environmental factors in affecting the temporal variations of NEE and NME; and (3) to quantify and compare the relative magnitude of each GHG budget and their net radiative forcing.

## 2. Materials and methods

### 2.1. Mariculture ponds and managements

The mariculture GHG flux tower in this study (23.9314°N, 117.4084°E) belongs to both ChinaFLUX and USCCC flux tower networks. It is built over algae-shellfish mariculture ponds in a subtropical estuarine wetland by Zhangjiang river of southeast China (Fig. 1), having a monsoon climate with a mean annual air temperature of 21.2 °C and mean annual precipitation of 1714.5 mm mostly occurring in spring and summer. The wetland experiences prevailing west-east wind direction and semidiurnal tidal cycle with a mean tidal range of ~2 m (Zhu et al., 2021a). Mariculture ponds in this wetland are comprised of paired algae and shellfish ponds (~1 m in depth), with razor clam (*Sinonovacula constricta*) as the dominant farming species. As one of the four major economic shellfish, razor clams are widely distributed along the Chinese coasts with total production up to  $8.6 \times 10^5$  t in 2020 (Fisheries Department of Agriculture Ministry of China, 2021). For each mariculture unit, there are two adjoining ponds respectively for razor clam and algae cultivations. These mariculture ponds are operated mainly with razor clam cultivation, occasionally supplemented with shrimp (*Penaeus*) and crab (*Scylla*). During the razor clam cultivation period, farmers regularly exchange pond water with tidal water via tidal cycles: at high tides, fresh tidal water is introduced into both algae and razor clam ponds with the former used for algae cultivation, while at low tides the razor clam pond is first drained and then filled with algae-rich water from the algae pond. After harvesting razor clams, the ponds are completely drained and set aside for around one week. During the shrimp/crab cultivation period, farmers feed shrimps and crabs in the ponds with aquatic feed pellets without intensive algae cultivation and water exchange activities.

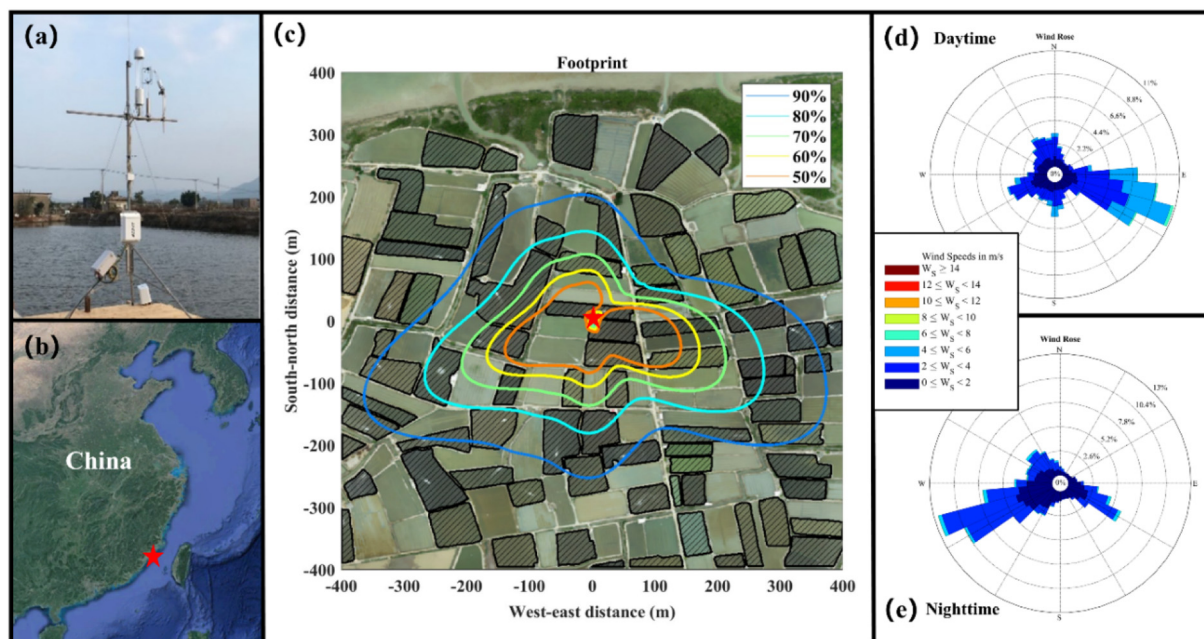


**Fig. 1.** The GHG eddy covariance flux measurement system (a) deployed over algae-shellfish mariculture ponds in a subtropical estuary of Southeast China (b). The algae (shaded) and shellfish ponds are shown with a UAV image (acquired on April 15, 2021), overlaid by the flux footprint climatology (c) (90% footprint area covers ~40 ponds). Daytime (d) and nighttime (e) wind rose plots are also shown. (For interpretation of the references to colour in this figure legend, the reader is referred to the web version of this article.)

On rainy days with possibly lower dissolved oxygen, farmers may operate paddlewheel aerators to improve the oxygen condition in the ponds.

## 2.2. GHG fluxes and ancillary measurements

Long-term continuous ecosystem-scale GHG fluxes including NEE and NME were measured by an EC system (Fig. 1a), consisting of two open-path gas analyzers of CO<sub>2</sub> (LI-7500, Li-COR Inc., Lincoln, NE, USA) and CH<sub>4</sub> (LI-7700, Li-COR Inc.) and a three-axis sonic anemometer (CSAT-3, Campbell Scientific, Inc., Logan, UT, USA). These sensors were deployed at a height of ~5 m above the mean water surface of mariculture ponds, and the footprint climatology analyses, using the algorithm of Kormann and Meixner (2001), confirmed that >90% of the fluxes were contributed by the ponds (~40 ponds) within 400 m around the tower (Fig. 1c). In order to ensure measurement quality of gas analyzers, we conducted instrument maintenance every half year including recalibration and refreshing drying chemicals. The sensor mirrors of the gas analyzers were also manually cleaned by a local farmer every one or two weeks to ensure accepted signal strength. Ancillary measurements include water temperature, wind speed and direction, photosynthetically active radiation (PAR), rainfall, and tidal salinity. Water temperature was measured using a HOBO U20L-04 Water Level Logger (Onset, Bourne, MA, USA) deployed in the pond with flux tower, and tidal salinity was measured using a HOBO U24-002-C Conductivity Logger (Onset) deployed in a nearby tidal creek. Wind speed and direction data were derived from raw measurements of the three-axis sonic anemometer. PAR and rainfall were respectively measured with a TE525MM Rain Gage (Campbell Scientific, Inc.) and a PQS1 PAR Quantum sensor (Kipp & Zonen, Delft, Netherlands) deployed on a nearby mangrove flux tower (~1 km away) (Zhu et al., 2021a). All ancillary measurements were converted to 30-min time series data for further analyses.

## 2.3. Flux processing and gap filling

A series of quality controls and flux calculations were implemented in the EddyPro 6.1 software (Li-COR Inc.) to produce 30-min time series data of NEE and NME from raw 10-Hz measurements (Zhu et al., 2021a; Zhu et al., 2021b). The 30-min flux data were discarded when rainfall

occurred or atmospheric mixing was insufficient with the friction velocity < 0.125 m s<sup>-1</sup> (Reichstein et al., 2005). The steady-state test and the developed turbulent condition test were applied to label flux time series with quality flags using the 0–1–2 system (Mauder et al., 2013), and those poor-quality fluxes with the quality flag of 2 were further discarded. The NME data with relative signal strength indicator <20% were also removed to avoid poor-quality data from potential contamination of LI-7700 mirrors. Data gaps within the time series of GHG fluxes resulted from quality controls and system malfunctions (a large gap occurred from January to March due to instrument failure). Over the one year, the percentages of valid 30-min NEE and NME data were 70.1% and 46.7%, respectively. The 30-min time series data were temporally aggregated to daily data, where those days with valid 30-min records less than 10 were excluded in the aggregation (leading to 25.0% missing for daily NME only). To examine annual GHG budgets and temporal variations across time scales, missing daily NME data were gap-filled using the artificial neural network (ANN) method (Liu et al., 2020; Zhu et al., 2021b) with three explanatory variables including water temperature, PAR, and tidal salinity (mean prediction error of the ANN model <15%).

## 2.4. Other calculations and data analyses

To examine the net climate effect from both NEE and NME of mariculture ponds, we applied the sustained-flux global warming potential (SGWP) metric (Neubauer and Megonigal, 2015; Liu et al., 2020) to compare the radiative forcing of NEE and NME. Two widely used time horizons of 20 and 100 years were selected to assess the net radiative forcing of NEE and NME, expressed as CO<sub>2</sub> equivalent (CO<sub>2</sub>-eq.; here 1 g CO<sub>2</sub>-C = 3.67 g CO<sub>2</sub>-eq.). The conversion values of 96 and 45 were used to calculate SGWP of CH<sub>4</sub> for 20-year and 100-year time horizons, respectively (Neubauer and Megonigal, 2015). To explore the contribution of algae ponds to GHG flux variations, we calculated a 30-min time series of area proportion of algae ponds (APAP) from temporally varying EC footprint coverage and corresponding land cover composition (algae pond, shellfish pond, and non-pond land), i.e., APAP was calculated every 30 min to indicate changing area proportion of algae ponds within the corresponding 90% footprint coverage. Statistical analyses including Pearson correlation and stepwise

regression were used to explore the potential contributions of various environmental factors to the GHG flux variations. The GHG values used in this study were indicated using the meteorological sign convention where negative and positive values denote downward and upward fluxes, respectively. Data processing and statistical analyses were mainly implemented using MATLAB software (MathWorks, Inc., Natick, MA, USA).

### 3. Results

#### 3.1. Temporal variations in environmental factors

The year-round time series of daily meteorological and hydrological data, including PAR, water temperature, tidal salinity, and rainfall, showed obvious seasonal variations in 2020 (Fig. 2). Daily PAR had both strong day-to-day and seasonal variations with daily cumulative PAR ranging from 3.64 to 59.15 mol m<sup>-2</sup> day<sup>-1</sup>. In comparison with PAR, water temperature had weaker day-to-day variations but an overall similar seasonal trend, with daily mean water temperature varying from 10.1 to 30.1 °C and the lowest and highest values occurring in January and July, respectively. Rainfall in this year mainly occurred in May (113.3 mm), June (216.6 mm), August (217.8 mm), and September (233.8 mm), with daily rainfall peaking at 104.8 mm. Daily mean tidal salinity ranged from 4.6 to 16.1 PSU (annual average of 11.8 PSU) with obvious down-regulation following rainfall events.

Mean diurnal variations of environmental factors (Fig. 3a-b) showed that 30-min PAR had a regular hump-shaped variation pattern peaking at 1267.3 μmol m<sup>-2</sup> s<sup>-1</sup> around noon. Tidal salinity had small diurnal fluctuations with the lowest and the highest values occurring at ~9 am and ~3 pm, respectively. Water temperature and wind speed shared similar diurnal variations with stronger values in the afternoon, respectively, peaking at 24.6 °C and 3.54 m s<sup>-1</sup> at ~4 pm. The wind regime is different between daytime and nighttime in this wetland, with the stronger eastern or south-eastern prevailing wind during daytime and weaker western or south-western prevailing wind during nighttime (Fig. 1d-e).

#### 3.2. Temporal variations in GHG fluxes

Mean diurnal variations of 30-min NEE and NME over algae-shellfish mariculture ponds differed both in the magnitude and variation pattern (Fig. 3c-d). The magnitude of mean 30-min NEE changed from -2.26 to 0.86 μmol m<sup>-2</sup> s<sup>-1</sup> with an average of -0.45 μmol m<sup>-2</sup> s<sup>-1</sup>. Over the day, mean NEE indicated a strong CO<sub>2</sub> sink (negative value) during daytime and a weak CO<sub>2</sub> source (positive value) during nighttime (Fig. 3c). In

contrast, NME indicated a CH<sub>4</sub> source over the day ranging from 0.0007 to 0.0093 μmol m<sup>-2</sup> s<sup>-1</sup> with an average of 0.0046 μmol m<sup>-2</sup> s<sup>-1</sup>. NME showed weaker diurnal variation with higher mean nighttime CH<sub>4</sub> emissions (0.0051 ± 0.0018 μmol m<sup>-2</sup> s<sup>-1</sup>) than mean daytime emissions (0.0041 ± 0.0015 μmol m<sup>-2</sup> s<sup>-1</sup>), although the difference was not statistically significant (Fig. 3d).

Over the year, algae-shellfish mariculture ponds acted as a CO<sub>2</sub> sink most of the time with daily NEE varying from -2.02 to 0.83 g CO<sub>2</sub>-C m<sup>-2</sup> day<sup>-1</sup> (averaged at -0.62 g CO<sub>2</sub>-C m<sup>-2</sup> day<sup>-1</sup>) (Fig. 4a). The ponds also acted as a CO<sub>2</sub> source at days during late May and from October to December. Monthly-mean daily NEE varied from -1.11 to -0.10 g CO<sub>2</sub>-C m<sup>-2</sup> day<sup>-1</sup> with higher CO<sub>2</sub> sinks in spring (-0.69 ± 0.17 g CO<sub>2</sub>-C m<sup>-2</sup> day<sup>-1</sup>) and summer (-0.95 ± 0.18 g CO<sub>2</sub>-C m<sup>-2</sup> day<sup>-1</sup>) than autumn (-0.37 ± 0.27 g CO<sub>2</sub>-C m<sup>-2</sup> day<sup>-1</sup>) and winter (-0.49 ± 0.35 g CO<sub>2</sub>-C m<sup>-2</sup> day<sup>-1</sup>), respectively. For NME, the ponds acted as a CH<sub>4</sub> source most of the time, with daily NME varying from -0.0080 to 0.0228 g CH<sub>4</sub>-C m<sup>-2</sup> day<sup>-1</sup> (averaged at 0.0039 g CH<sub>4</sub>-C m<sup>-2</sup> day<sup>-1</sup>) and monthly-mean daily NME varying from 0.0002 to 0.0117 g CH<sub>4</sub>-C m<sup>-2</sup> day<sup>-1</sup> (Fig. 4b). The CH<sub>4</sub> emissions from the ponds were much higher in spring (0.0052 ± 0.0028 g CH<sub>4</sub>-C m<sup>-2</sup> day<sup>-1</sup>) and summer (0.0067 ± 0.0044 g CH<sub>4</sub>-C m<sup>-2</sup> day<sup>-1</sup>), while NME in autumn (0.0036 ± 0.0014 g CH<sub>4</sub>-C m<sup>-2</sup> day<sup>-1</sup>) and winter (0.0005 ± 0.0003 g CH<sub>4</sub>-C m<sup>-2</sup> day<sup>-1</sup>) fluctuated more with a few days acting as a CH<sub>4</sub> sink.

#### 3.3. Correlations between GHG fluxes and environmental factors

Correlations between GHG fluxes over algae-shellfish mariculture ponds and related environmental factors were analyzed across different time scales. Daytime and nighttime 30-min NEE were, respectively, negatively and positively correlated with water temperature (Fig. 5a). In contrast, daytime and nighttime 30-min NEE were, positively and negatively correlated with tidal salinity (Fig. 5b). For all daytime and nighttime data, 30-min NEE was negatively and positively correlated with water temperature and tidal salinity, respectively. For 30-min NME, both daytime and nighttime fluxes were positively correlated with water temperature but negatively correlated with tidal salinity, and there was no obvious difference in these correlations between daytime and nighttime periods (Fig. 5c-d).

The potential effects of wind speed and APAP on GHG fluxes over algae-shellfish mariculture ponds were explored using 30-min data (Fig. 6). The magnitude of 30-min wind speed varied from 0.24 to 5.61 m s<sup>-1</sup> (average

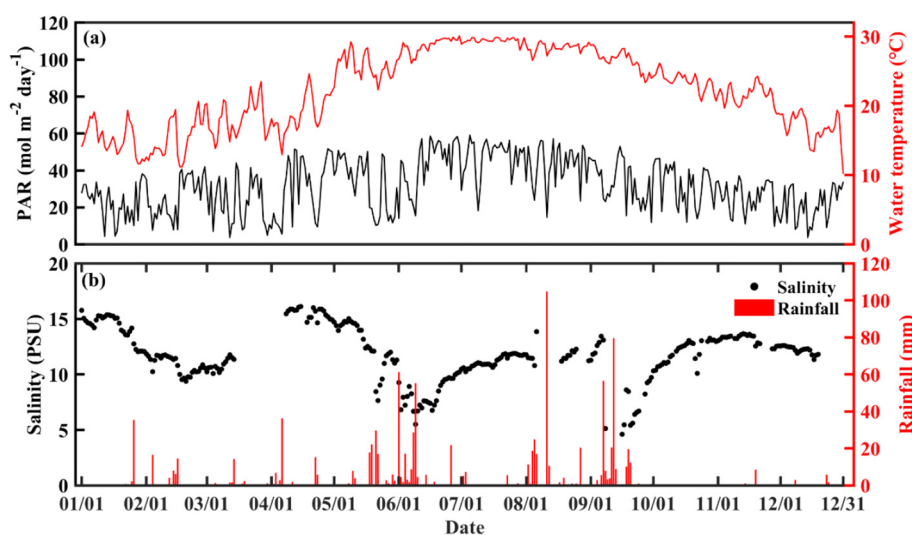


Fig. 2. Temporal variations in daily environmental factors in 2020, including (a) cumulative photosynthetically active radiation (PAR), mean water temperature, (b) mean tidal salinity, and cumulative rainfall.

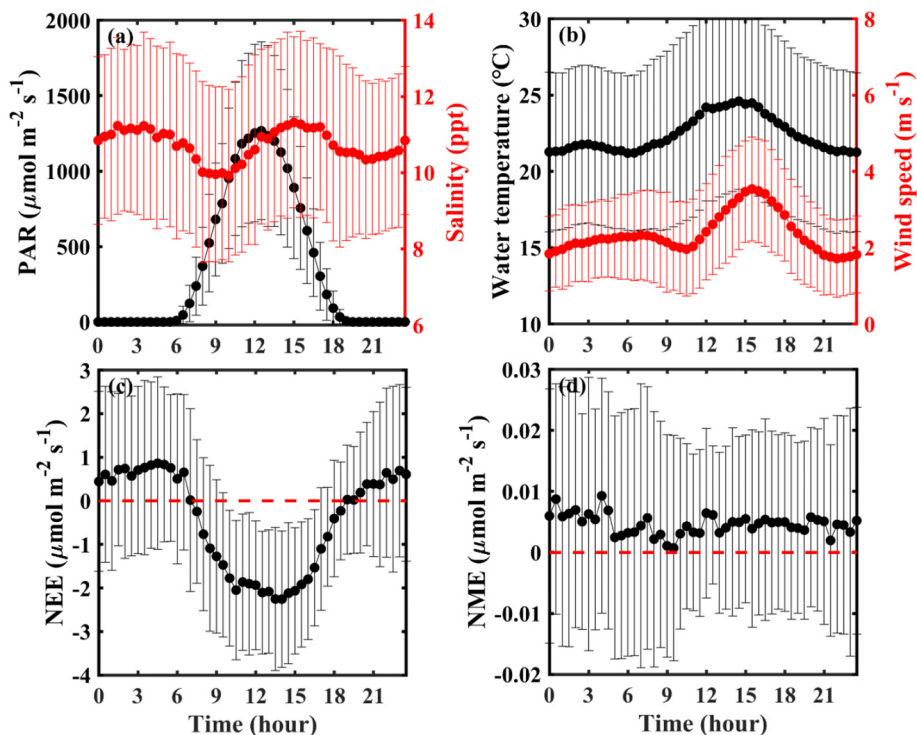


Fig. 3. Mean diurnal variations and standard deviations of 30-min environmental factors including (a) photosynthetically active radiation (PAR) and tidal salinity, (b) water temperature and wind speed, as well as (c) net CO<sub>2</sub> exchange (NEE) and (d) net CH<sub>4</sub> exchange (NME) over algae-shellfish mariculture ponds.

of 2.35 m s<sup>-1</sup>) and the magnitude of 30-min APAP varied from 0.26 to 0.61 (average of 0.43). All of the 30-min time series of wind speed, APAP, and GHG fluxes shared overall similar diurnal and seasonal variations, having stronger values in the afternoon. Further statistical analysis showed that the correlation between all 30-min NEE (y) and APAP (x) was statistically significant and negative ( $y = -3.6x + 0.93, R^2 = 0.017, p < 0.05$ )

(Fig. 7a). By grouping daily values of NEE-APAP correlation coefficients by different PAR levels (aiming to minimize the impacts of PAR on NEE), the median values of correlation coefficients fluctuated from -0.19 to 0.03 with better correlations at higher levels of PAR (Fig. 7c). The correlation between all 30-min NME (y) and APAP (x) was statistically significant and positive ( $y = 0.016x - 0.0023, R^2 = 0.005, p < 0.05$ ) (Fig. 7b). By

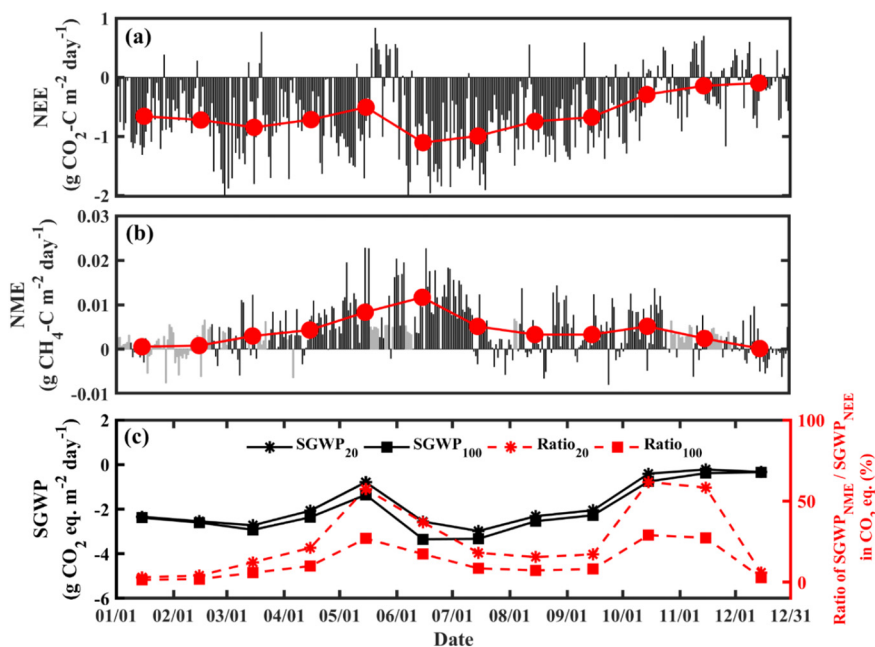
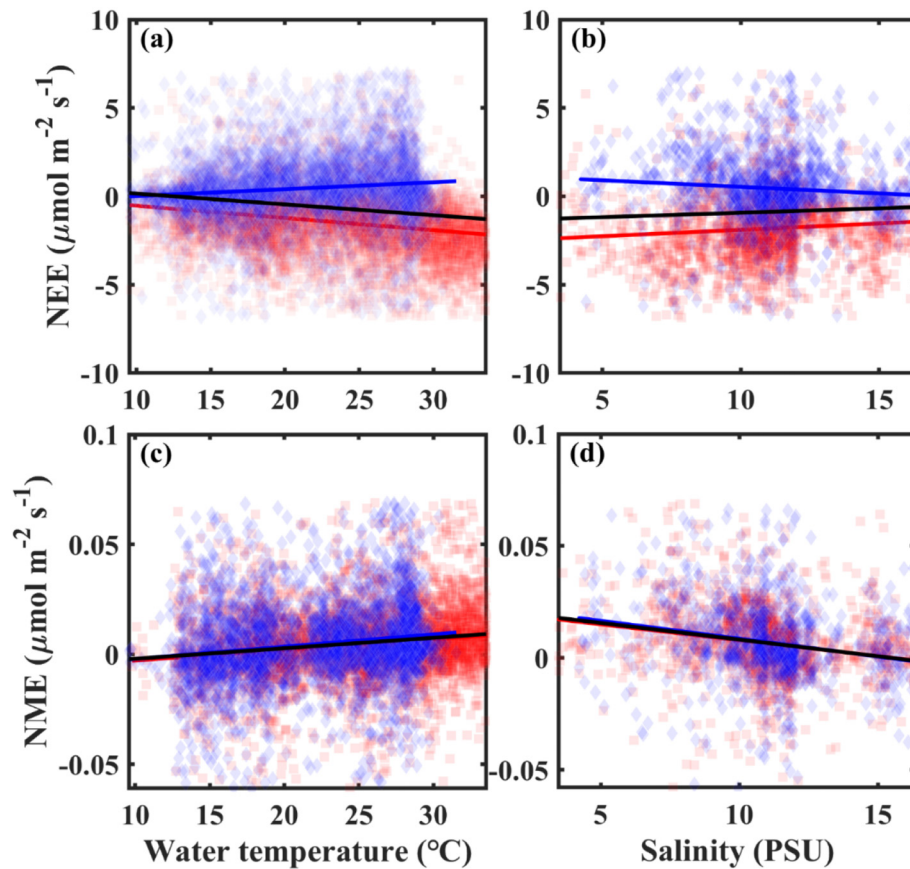


Fig. 4. Seasonal variations in daily (bars) and monthly (dots) (a) net CO<sub>2</sub> exchange (NEE) and (b) net CH<sub>4</sub> exchange (NME) in 2020 over algae-shellfish mariculture ponds. The gray bars denote the gap-filled daily values from the ANN model simulations. Monthly variations in sustained-flux global warming potential (SGWP) and the ratio of NEE-induced SGWP offset by NME are also shown for both 20-year and 100-year time horizons.



**Fig. 5.** Relationships between 30-min GHG fluxes (net CO<sub>2</sub> exchange (NEE) and net CH<sub>4</sub> exchange (NME)) and two key environmental factors (water temperature and tidal salinity). Data are grouped by daytime (red) and nighttime (blue) periods with corresponding fitting lines, while the black lines denote the fitted relationships using the whole data. All linear relationships are statistically significant at  $p < 0.05$ . (For interpretation of the references to colour in this figure legend, the reader is referred to the web version of this article.)

grouping daily values of NME-APAP correlation coefficients by different temperature levels (aiming to minimize the impacts of temperature on NME), the median values of correlation coefficients fluctuated from  $-0.07$  to  $0.15$  with better correlations at higher levels of water temperature (Fig. 7d).

Correlation analyses indicated that (Fig. 8), for 30-min data, there were negative correlations (statistically significant at  $p < 0.05$ ) between NEE and PAR (Pearson correlation coefficient:  $-0.62$ ), water temperature ( $-0.23$ ), and APAP ( $-0.20$ ). Similarly, for daily data, NEE was negatively correlated ( $p < 0.05$ ) with PAR ( $-0.51$ ), APAP ( $-0.42$ ), water temperature ( $-0.23$ ),

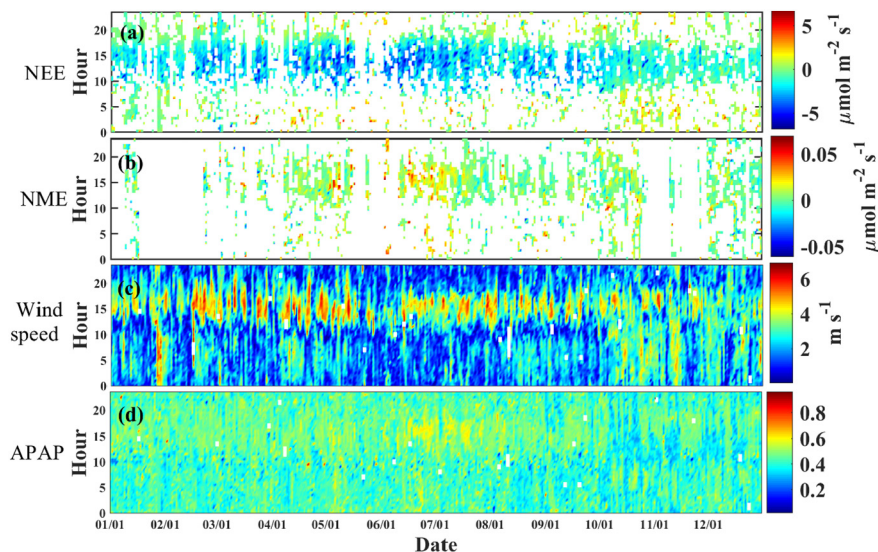


**Fig. 6.** Temporal variations in 30-min measurements of (a) net CO<sub>2</sub> exchange (NEE), (b) net CH<sub>4</sub> exchange (NME), (c) area proportion of algae ponds (APAP), and (d) wind speed. White area denotes missing data due to instrument failure or quality controls.

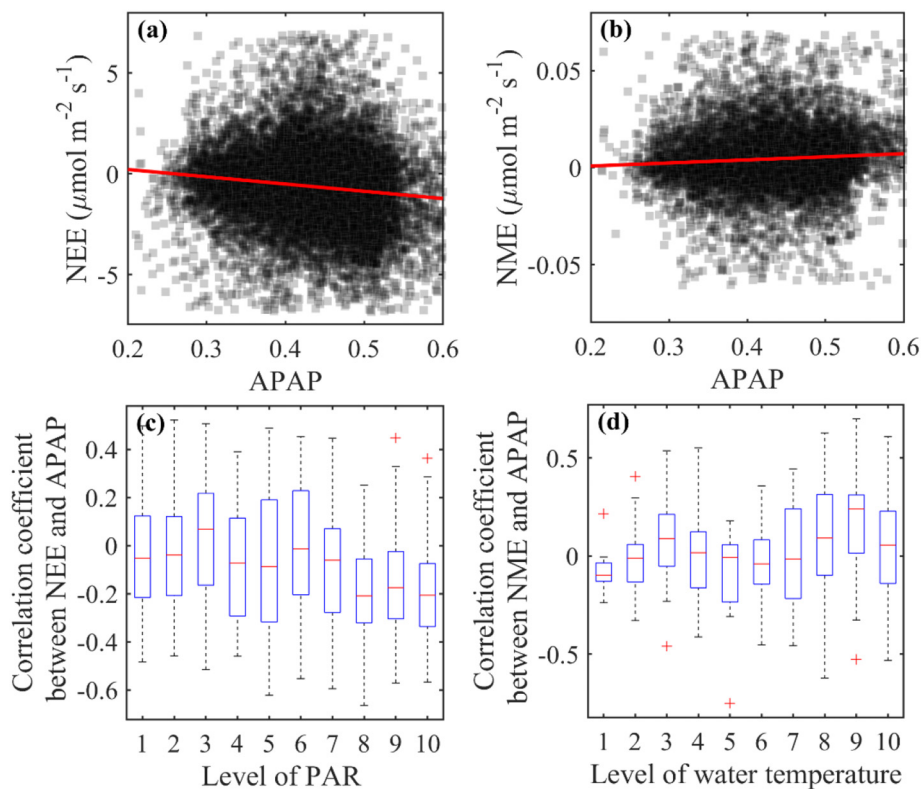


**Fig. 7.** Relationships between 30-min GHG fluxes (net CO<sub>2</sub> exchange (NEE) and net CH<sub>4</sub> exchange (NME)) and area proportion of algae ponds (APAP) with corresponding fitting lines (a and b). The changes of daily GHG-APAP correlations with two key environmental factors of (c) photosynthetically active radiation (PAR) and (d) water temperature are shown using boxplots, in which daily values of GHG-APAP correlation coefficient based on 30-min data are grouped by ten incremental levels of each environmental factor.

but positively correlated ( $p < 0.05$ ) with tidal salinity (0.14). Stepwise regression analyses also confirmed that the variations in 30-min NEE could be explained by the combination of PAR, water temperature (Tw), and APAP:  $NEE = 0.58 - 0.002PAR + 0.026Tw - 2.4APAP$  ( $R^2 = 0.39$ ). In comparison with NEE, the correlations between NME and these environmental factors were overall weaker for both 30-min and daily data. NME was negatively correlated ( $p < 0.05$ ) with tidal salinity ( $-0.22$  and  $-0.15$  for 30-min and daily data, respectively) and positively correlated ( $p < 0.05$ ) with water temperature (0.20 and 0.35), PAR (0.06 and 0.24), and APAP (0.13 and 0.23). Stepwise regression analyses confirmed that the variations in 30-min NME could

be explained by the combination of salinity, water temperature (Tw), and APAP:  $NME = 0.0022 - 0.0011Sal + 0.0003Tw + 0.0164APAP$  ( $R^2 = 0.07$ ).

### 3.4. Temporal variations in global warming potential

Using the SGWP as a metric to assess the net climate effect from NEE and NME over the mariculture ponds, monthly-mean SGWP ranged from  $-2.98$  to  $-0.22$  g CO<sub>2</sub>-eq. m<sup>-2</sup> day<sup>-1</sup> for 20-year time horizon and from  $-3.35$  to  $-0.34$  g CO<sub>2</sub>-eq. m<sup>-2</sup> day<sup>-1</sup> for 100-year time horizon

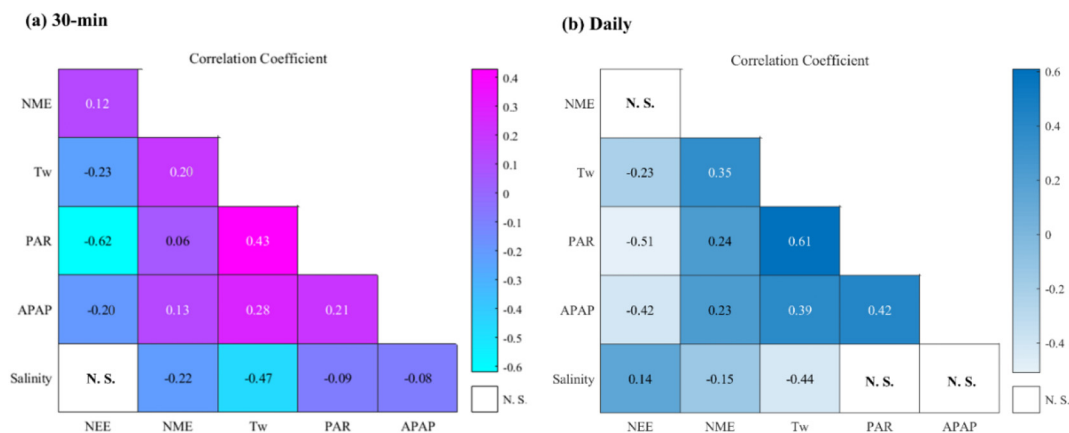


**Fig. 8.** Heatmaps of Pearson correlation coefficients between (a) 30-min and (b) daily GHG fluxes (net CO<sub>2</sub> exchange (NEE) and net CH<sub>4</sub> exchange (NME)) and environmental factors, including water temperature (Tw), photosynthetically active radiation (PAR), area proportion of algae ponds (APAP), and tidal salinity. All shown correlation coefficients are statistically significant with  $p < 0.05$  (N. S. means not significant).

(Fig. 4c). During most of the time over the study period, the NME-induced warming effect partially offset the NEE-induced cooling effect. The SGWP ratio of monthly NME over NEE, or the CH<sub>4</sub> offset potential, varied from 2.97% to 61.76% for a 20-year time horizon and from 1.39% to 28.95% over a 100-year time horizon. Over the year, monthly CH<sub>4</sub> offset potential had two peaks in May and October–November. For annual GHG budgets, the mariculture ponds acted as a CO<sub>2</sub> sink of  $-227.69 \text{ g CO}_2\text{-C m}^{-2} \text{ year}^{-1}$  and a CH<sub>4</sub> source of  $1.44 \text{ g CH}_4\text{-C m}^{-2} \text{ year}^{-1}$ , together leading to annual SGWP of  $-650.1$  and  $-746.3 \text{ g CO}_2\text{-eq. m}^{-2} \text{ year}^{-1}$  for 20-year and 100-year time horizons, respectively (Table 1).

#### 4. Discussion

Temporal or spatial variations of water-air GHG fluxes have been reported in different aquatic ecosystems including mariculture/freshwater ponds, reservoirs, lakes, rivers, and wetlands (Chen et al., 2016b; Gerardo-Nieto et al., 2017; Van Dam et al., 2021). The farming types and management modes are the key factors of regulating carbon budgets in aquaculture ecosystems (Yuan et al., 2019). Among these aquaculture ecosystems, mariculture ecosystems tend to have stronger temporal and spatial variations due to more intensive impacts from natural and human factors (Yang et al., 2019b). Long-term continuous and high-frequency EC measurements in this study confirmed that both NEE and NME showed strong diurnal and seasonal variations.

Mean diurnal variations of NEE in this study indicated a much stronger daytime CO<sub>2</sub> sink than a nighttime CO<sub>2</sub> source over algae-shellfish

mariculture ponds, which is different from many previous studies on aquatic ecosystems showing a CO<sub>2</sub> source over the day (Table 1). The diurnal variations of CO<sub>2</sub> fluxes over mariculture ponds are mainly associated with the photosynthesis and respiration processes of algae and shellfish (Delille et al., 2009; Jiang et al., 2013). Different from most mariculture pond studies showing stronger CO<sub>2</sub> emissions in hotter summer and autumn (Chen et al., 2016b; Chen et al., 2018), the algae-shellfish mariculture ponds in this study had consistent monthly CO<sub>2</sub> sink peaking in summer. Compared with other studies on reservoirs (Zhao et al., 2013), lakes (Vallejo et al., 2021), and rivers (Teodoru et al., 2015), these algae-shellfish mariculture ponds had a stronger CO<sub>2</sub> sink capacity across the air-water interface. In this study region, around half of the ponds were reserved for algae cultivation with management efforts, and thus the carbon fixed by algae photosynthesis might be much greater than other types of aquatic ecosystems. The biotic calcification of shellfish could also contribute to improving the air-water CO<sub>2</sub> sink capacity in these ponds (Turolla et al., 2020).

Mean diurnal variations of NME over these algae-shellfish mariculture ponds with higher nighttime emissions are consistent with Zhang et al. (2019) showing higher nighttime CH<sub>4</sub> emissions in lakes but different from Hu et al. (2020a) showing lower nighttime CH<sub>4</sub> emissions in mariculture ponds. The temporal variability of NME is co-regulated by many processes including CH<sub>4</sub> production, oxidation, and transport (Rutegwa et al., 2019). Aquaculture management such as feeding and water exchange activities will greatly affect these processes (Chen et al., 2018; Yang et al., 2019b), resulting in strong variations in NME under different management

**Table 1**

Flux measurements and varying ranges (in brackets if any) of net CO<sub>2</sub> exchange (NEE) and net CH<sub>4</sub> exchange (NME) at the air-water interface of different aquatic ecosystems, as well as corresponding sustained-flux global warming potential (SGWP) using 20-year and 100-year time horizons.

Ecosystem	Type	Period	NEE g CO <sub>2</sub> -C m <sup>-2</sup> day <sup>-1</sup>	NME mg CH <sub>4</sub> -C m <sup>-2</sup> day <sup>-1</sup>	SGWP g CO <sub>2</sub> -eq. m <sup>-2</sup> year <sup>-1</sup>		Reference
					20-year	100-year	
Mariculture pond	Razor clam	2020.01–2020.12	-0.62 (-2.02 – 0.38)	3.90 (8.00– 22.80)	-650.1	-746.3	this study
	Crab/shrimp	2014.07–2014.11	-0.18 (-0.46 – 0.27)	1.19 (0.39– 2.59)	-182.3	-211.3	Zhang et al. (2020a)
	Crab/shrimp/clam	2014.07–2014.11	0.44 (0.16– 0.64)	1.24 (0.20– 2.50)	639.8	609.5	Zhang et al. (2020a)
	Shrimp	2015.06–2015.10	0.11 (-0.42– 0.54)	1548.18 (99.54– 3408.84)	71,491.1	33,591.6	Yang et al. (2018b)
	Shrimp	2015.06–2015.10	0.10 (-0.06– 0.38)	173.52 (45.72– 423.72)	8128.9	3881.1	Yang et al. (2018b)
Freshwater pond	Fish	2013.07–2013.09	0.78 (-0.23– 2.41)	167.77 (11.20– 869.25)	8766.9	4660.0	Zhu et al. (2016)
	Grass carp	2014.05–2014.09	0.41 (0.13– 0.81)	15.96 (3.00– 63.48)	1278.9	888.2	Xiong et al. (2017)
	/	2010.06–2010.10	0.10 (0.04– 0.18)	15.60 (3.60– 42.00)	845.6	463.7	Natchimuthu et al. (2014)
Reservoir	/	2014.10–2015.06	0.15 (0.14– 0.16)	6.12 (1.08– 15.84)	479.7	329.9	Gerardo-Nieto et al. (2017)
	/	2010.01–2010.12	1.57 (1.06– 2.10)	4.32 (0.36– 6.84)	2270.9	2165.2	Zhao et al. (2013)
	/	2009.04–2010.01	0.16 (-0.24– 0.46)	58.80 (3.60– 142.80)	2918.6	1479.2	Chanudet et al. (2011)
Lake	/	2012.05–2012.09	6.12 (-0.60– 24.36)	100.80 (-2.88– 720.00)	12,723.3	10,255.7	Crawford et al. (2014)
	/	2014.10–2015.06	0.25 (-0.28– 0.60)	0.54 (1.08– 17.28)	359.4	346.2	Gerardo-Nieto et al. (2017)
	/	2018.03–2018.09	0.04 (-0.03– 0.18)	0.10 (0.03– 0.59)	55.9	53.6	Vallejo et al. (2021)
Wetland	Saltmarsh	2012.04–2012.11	4.24 (0.10– 21.97)	11.52 (5.76– 115.20)	6126.8	5844.8	Olsson et al. (2015)
	/	2011.03–2013.11	0.51 (-1.15– 4.61)	1.44 (-7.92– 20.64)	744.3	709.1	Shiau et al. (2016)
	/	2012.01–2013.01	-0.45 (-0.67 ~ -0.31)	14.40 (0.00– 72.00)	66.7	-285.8	Wilson et al. (2015)
River	/	2014–2015	3.45 (0.62– 14.26)	53.40 (-12.00– 1635.80)	7017.3	5710.1	Qu et al. (2017)
	/	2003–2004	5.40 (0.07– 14.30)	66.00 (3.20– 120.00)	10,169.3	8553.6	Silvennoinen et al. (2008)
	/	2012–2013	3.38	48.50	6696.5	5509.2	Teodoru et al. (2015)

scenarios. Daytime lower net CH<sub>4</sub> emissions in this study could result from stronger CH<sub>4</sub> oxidation with more dissolved oxygen from algae photosynthesis, while nighttime higher emissions were associated with weaker CH<sub>4</sub> oxidation (Liu et al., 2016). The seasonal cycle of NME showed that CH<sub>4</sub> emissions in summer and spring were remarkably higher than in winter, which is in accordance with previous findings that seasonal variations of CH<sub>4</sub> emissions were temperature-controlled (Xing et al., 2005; Villa et al., 2019). The mean daily NME in these mariculture ponds (0.0039 g CH<sub>4</sub>-C m<sup>-2</sup> day<sup>-1</sup>) fell within the varying range (0.0001–1.548 g CH<sub>4</sub>-C m<sup>-2</sup> day<sup>-1</sup>) among aquatic ecosystems (Table 1). The CH<sub>4</sub> emission rates in algae-shellfish ponds of this study were much lower than chamber-based CH<sub>4</sub> emissions in shrimp ponds experiencing similar subtropical climates (Yang et al., 2019b). On the one hand, the direct feeding process in shrimp ponds could lead to higher CH<sub>4</sub> emissions than razor clam farming feed by algae cultivation. On the other hand, chamber-based measurements with limited sampling locations could suffer from spatial representation issues and have large uncertainty given that CH<sub>4</sub> fluxes varied spatially between and within mariculture ponds (Yang et al., 2019b).

The strong diurnal, day-to-day and seasonal variations of GHG fluxes in this study and previous studies (Morin et al., 2014; Hu et al., 2020a) imply that discrete flux measurements (often made during farming season and daytime periods) by traditional chamber-based methods cannot fully capture the temporal dynamics of GHG fluxes and could thus result in large bias in representing GHG budgets. It is worth noting that, in late May, the ponds of this study acted as a CO<sub>2</sub> source and a lower CH<sub>4</sub> source over the sustained drainage period after harvesting razor clam, which is consistent with the previous finding that drainage transforms mariculture ponds from a CO<sub>2</sub> sink to a source (Yang et al., 2018a). Both NEE and NME showed great fluctuation from November to December, which could result from more frequent human management activities at the early stage of razor clam cultivation.

The consistent and negative monthly SGWP for both 20-year and 100-year time horizons confirmed that these algae-shellfish mariculture ponds exerted a net cooling radiative effect in 2020, which is different from most previous GHG studies on aquatic ecosystems showing net warming radiative effects (Table 1). As an aquatic ecosystem, this net cooling radiative effect of the mariculture ponds is substantial with the magnitude accounting for ~20% of the cooling effect of mangrove ecosystems (right next to the ponds) estimated with the same EC approach (Zhu et al., 2021b). The monthly SGWP ratio of NEE over NME varied a lot over the year due to asynchronous seasonal variations in NEE and NME. This highlights the importance and necessity of conducting long-term and continuous GHG flux measurements to cover both short-term and long-term temporal variations.

The Pearson correlation and stepwise regression analyses confirmed that the GHG fluxes over these algae-shellfish ponds were mainly affected by PAR, water temperature, salinity, and APAP. In algae-rich aquatic ecosystems as in this study, PAR is the dominant environmental control of NEE, since temporal variations in NEE are mainly regulated by algae photosynthesis (Delille et al., 2009; Jiang et al., 2013). PAR may also indirectly affect daytime NME since stronger photosynthesis with more PAR can promote dissolved oxygen and resultant CH<sub>4</sub> oxidation (Bridgman et al., 2013). The strong correlations between GHG fluxes and water temperature confirm the important role of water temperature in regulating GHG fluxes, which is consistent with the previous finding that thermal conditions strongly affect GHG fluxes over aquaculture ponds (Wu et al., 2018; Shafer et al., 2020). The magnitude of daytime CO<sub>2</sub> sink and nighttime CO<sub>2</sub> source increased with water temperature. During the daytime, stronger photosynthesis stimulated by higher water temperature promotes CO<sub>2</sub> sink, while, during nighttime, higher water temperature promotes CO<sub>2</sub> emissions by stimulating the mineralization process (Gruca-Rokosz et al., 2017; Villa et al., 2019). Water temperature is the key environmental factor of NME. On the one hand, a higher temperature can stimulate methanogenesis processes in water and sediment, and thus promote CH<sub>4</sub> production (Bridgman et al., 2013). On the other hand, a higher temperature can enhance CH<sub>4</sub> emission rates via diffusion and ebullition pathways (DelSontro et al., 2016). Both NEE and NME were correlated with tidal salinity with CH<sub>4</sub>

emissions more inhibited by increasing salinity, which agrees with previous findings on the negative impacts of salinity on photosynthetic efficiency (Barr et al., 2013) and CH<sub>4</sub> emissions (Hu et al., 2020b). The negative APAP-NEE and positive APAP-NME correlations suggested that temporally varying APAP also partially explained the variations in GHG fluxes over these algae-shellfish ponds, which is consistent with the study demonstrating the carbon sequestration capacity of algae in aquaculture ponds (Anikuttan et al., 2016).

It is important to note that current EC-based assessments of air-water GHG fluxes are different from complete mariculture carbon balance analyses, which should also consider other life-cycle carbon input/output components such as farming, harvest, and consumption (Guo et al., 2017). Due to the lack of many other measurements, we're not able to conduct a carbon balance analysis in current study, which only focuses on air-water GHG fluxes. However, we do collect some information to estimate the amount of harvested carbon, which can be compared with the EC-based carbon measurements in the context of the whole carbon balance. For the paired algae and shellfish ponds (~2500 m<sup>2</sup> for each) where the flux tower locates, annual wet height of harvested razor clam is ~10,000 kg from the shellfish pond (personal communication), which can be converted to a land area-based harvested carbon value of 246 g C m<sup>-2</sup> year<sup>-1</sup> (10000kg × 1000g/kg × 0.41 × 0.30/2500m<sup>2</sup>/2) by assuming a dry-wet ratio of 41% and a carbon concentration of 30% for razor clam (Guo et al., 2017). This harvested carbon value is only slightly larger than EC-based algae carbon input (227.7 g C m<sup>-2</sup> year<sup>-1</sup>). By assuming algae carbon input and harvested carbon removal are the two largest flux components (Guo et al., 2017) and almost all harvested carbon will finally release back to the atmosphere, we can infer that this mariculture ecosystem might be near carbon neutral from the perspective of life-cycle carbon balance.

The data measurements and analyses of this study suffer from several limitations. First, although the EC-based long-term continuous measurements can well capture the strong seasonal variations in GHG fluxes, these EC-based fluxes also have uncertainties mainly from data gaps, flux corrections, and quality controls. Future simultaneous flux measurements from EC and other methods like chamber-based ones are needed to improve the assessment of GHG budgets. Second, we were not able to fully assess the GHG budgets over the algae-shellfish ponds due to the lack of long-term measurements of other GHG fluxes like N<sub>2</sub>O. The incorporation of N<sub>2</sub>O flux is needed in future studies since N<sub>2</sub>O flux might be also important in human-managed mariculture ponds with abundant nutrient loadings (Yang et al., 2020a; Yuan et al., 2021). Third, the EC flux measurements only represented net GHG exchange across the water-air interface of mariculture ponds, which resulted from a series of GHG production, transport, and consumption processes across different interfaces within the ponds. More ancillary measurements including water quality data such as chlorophyll and pH are needed to better determine the environmental controls of net GHG fluxes. Lastly, the biotic disturbances from razor clam should be also considered in future studies to better analyze the temporal variations of GHG fluxes, since the disturbances from biotic activities like drilling could affect sediment micro-environment and GHG production (Oliveira-Junior et al., 2019).

## 5. Conclusions

The EC-based high-frequency continuous measurements of one-year air-water GHG fluxes over algae-shellfish mariculture ponds suggested that, in 2020, these ponds acted as a strong CO<sub>2</sub> sink of -227.69 g CO<sub>2</sub>-C m<sup>-2</sup> year<sup>-1</sup> and a weak CH<sub>4</sub> source of 1.44 g CH<sub>4</sub>-C m<sup>-2</sup> year<sup>-1</sup>, leading to net GHG sinks of -650.1 and -746.3 g CO<sub>2</sub>-eq. m<sup>-2</sup> year<sup>-1</sup> (expressed using the SGWP metric) at 20-year and 100-year time horizons, respectively. The year-round consistent CO<sub>2</sub> uptake over the ponds dominated this net GHG cooling effect, while annually the NME-induced warming effect offset 25.9% (20-year) and 12.1% (100-year) of the NEE-induced cooling effect. On the diurnal scale, NEE showed regular transitions between the daytime sink and nighttime source, while NME had no regular

varying pattern. On the seasonal scale, NEE and NME had different varying patterns but both of them tended to be stronger in the sink/source capacity in summer and more fluctuating in winter. Among environmental factors, NEE and NME tended to be more regulated by PAR and salinity, respectively, but both of them were affected by water temperature and area proportion of algae ponds. This study confirms that the algae-shellfish mariculture ponds are GHG hotspots of both CO<sub>2</sub> and CH<sub>4</sub> fluxes, and they act as a net GHG sink due to much stronger CO<sub>2</sub> uptake than CH<sub>4</sub> emissions across the air-water interface. Strong diurnal and seasonal variations in both GHG fluxes and their net radiative forcing highlights the necessity of conducting long-term and continuous measurements of air-water GHG fluxes over algae-shellfish mariculture ponds. To the best of our knowledge, this is the first study to explore spatio-temporal dynamics of multiple GHG fluxes over algae-shellfish mariculture ponds based on high-frequency EC measurements; however, multiple-year continuous data records of air-water GHG fluxes, environmental factors, and related human activities are highly needed in future studies to improve the assessment of the climate benefits of mariculture ponds.

### CRedit authorship contribution statement

**Yiping Zhang:** Data curation, Formal analysis, Investigation, Methodology, Visualization. **Zhangcai Qin:** Formal analysis, Methodology, Writing – review & editing. **Tingting Li:** Formal analysis, Methodology, Writing – review & editing. **Xudong Zhu:** Conceptualization, Formal analysis, Funding acquisition, Investigation, Methodology, Project administration, Supervision, Validation, Visualization, Writing – original draft, Writing – review & editing.

### Declaration of competing interest

The authors declare that they have no known competing financial interests or personal relationships that could have appeared to influence the work reported in this paper.

### Acknowledgments

We are grateful to members from Coastal Ecology & Remote Sensing Lab led by Dr. Xudong Zhu at Xiamen University and staff at Zhangjiang Estuary Mangrove National Nature Reserve for their help in the fieldwork. This research was funded by the Special Project on National Science and Technology Basic Resources Investigation of China (2021FY100704), the Natural Science Foundation of Fujian Province, China (2020J01112079), the Youth Innovation Foundation of Xiamen, China (3502Z20206038), and the Fundamental Research Funds for the Central Universities of China (20720210075).

### References

Aime, J., Allenbach, M., Bourgeois, C., et al., 2018. Variability of CO<sub>2</sub> emissions during the rearing cycle of a semi-intensive shrimp farm in a mangrove coastal zone (New Caledonia). *Mar. Pollut. Bull.* 129 (1), 194–206.

Anikuttan, K.K., Adhikari, S., Kavitha, M., et al., 2016. Carbon sequestration capacity of sediments, algae, and zooplankton from fresh water aquaculture ponds. *Environ. Monit. Assess.* 188 (7).

Baldocchi, D.D., 2020. How eddy covariance flux measurements have contributed to our understanding of global change biology. *Glob. Chang. Biol.* 26 (1), 242–260.

Barr, J.G., Engel, V., Fuentes, J.D., et al., 2013. Modeling light use efficiency in a subtropical mangrove forest equipped with CO<sub>2</sub> eddy covariance. *Biogeosciences* 10 (3), 2145–2158.

Bridgman, S.D., Cadillo-Quiroz, H., Keller, J.K., et al., 2013. Methane emissions from wetlands: biogeochemical, microbial, and modeling perspectives from local to global scales. *Glob. Chang. Biol.* 19, 1325–1346.

Chanudet, V., Descloux, S., Harby, A., et al., 2011. Gross CO<sub>2</sub> and CH<sub>4</sub> emissions from the Nam Ngum and Nam Leuk sub-tropical reservoirs in Lao PDR. *Sci. Total Environ.* 409 (24), 5382–5391.

Chen, Y., Dong, S., Wang, F., et al., 2016a. Carbon dioxide and methane fluxes from feeding and no-feeding mariculture ponds. *Environ. Pollut.* 212, 489–497.

Chen, Y., Dong, S., Wang, Z., et al., 2016. Variations in CO<sub>2</sub> fluxes from grass carp *Ctenopharyngodon idella* aquaculture polyculture ponds. *Aquac. Environ. Interact.* 8, 31–40.

Chen, Y., Dong, S., Bai, Y., et al., 2018. Carbon budgets from mariculture ponds without a food supply. *Aquacult. Environ. Interact.* 10, 465–472.

Crawford, J.T., Lottig, N.R., Stanley, E.H., et al., 2014. CO<sub>2</sub> and CH<sub>4</sub> emissions from streams in a lake-rich landscape: patterns, controls, and regional significance. *Glob. Biogeochem. Cycl.* 28 (3), 197–210.

Delille, B., Borges, A.V., Delille, D., 2009. Influence of giant kelp beds (*Macrocystis pyrifera*) on diel cycles of pCO<sub>2</sub> and DIC in the sub-Antarctic coastal area. *Estuar. Coast. Shelf Sci.* 81 (1), 114–122.

DelSontro, T., Boutet, L., St-Pierre, A., et al., 2016. Methane ebullition and diffusion from northern ponds and lakes regulated by the interaction between temperature and system productivity. *Limnol. Oceanogr.* 61, S62–S77.

Erkkila, K.M., Ojala, A., Bastviken, D., et al., 2018. Methane and carbon dioxide fluxes over a lake: comparison between eddy covariance, floating chambers and boundary layer method. *Biogeosciences* 15 (2), 429–445.

Fisheries Department of Agriculture Ministry of China, 2021. 2021 China Fishery Statistical Yearbook.

Gao, Y., Jia, J., Lu, Y., et al., 2020. Determining dominating control mechanisms of inland water carbon cycling processes and associated gross primary productivity on regional and global scales. *Earth Sci. Rev.* 103497.

Gerardo-Nieto, O., Astorga-Espana, M.S., Mansilla, A., et al., 2017. Initial report on methane and carbon dioxide emission dynamics from sub-Antarctic freshwater ecosystems: a seasonal study of a lake and a reservoir. *Sci. Total Environ.* 593, 144–154.

Gruca-Rokosz, R., Bartoszek, L., Koszelnik, P., 2017. The influence of environmental factors on the carbon dioxide flux across the water-air interface of reservoirs in South-Eastern Poland. *J. Environ. Sci.* 56, 290–299.

Guo, K., Zhao, W., Jiang, Z., et al., 2017. A study of organic carbon, nitrogen and phosphorus budget in jellyfish-shellfish-fish-prawn polyculture ponds. *Aquac. Res.* 48 (1), 68–76.

Holgerson, M.A., 2015. Drivers of carbon dioxide and methane supersaturation in small, temporary ponds. *Biogeochemistry* 124 (1–3), 305–318.

Hu, B., Xu, X., Zhang, J., et al., 2020a. Diurnal variations of greenhouse gases emissions from reclamation mariculture ponds. *Estuar. Coast. Shelf Sci.* 237.

Hu, M.J., Sardans, J., Yang, X.Y., et al., 2020b. Patterns and environmental drivers of greenhouse gas fluxes in the coastal wetlands of China: a systematic review and synthesis. *Environ. Res.* 186, 10.

IPCC, 2021. Summary for policymakers. In: Masson-Delmotte, V., Zhai, P., Pirani, A., Connors, S.L., Péan, C., Berger, S., Caud, N., Chen, Y., Goldfarb, L., Gomis, M.I., Huang, M., Leitzell, K., Lonnoy, E., Matthews, J.B.R., Maycock, T.K., Waterfield, T., Yeleki, O., Yu, R., Zhou, B. (Eds.), *Climate Change 2021: The Physical Science Basis. Contribution of Working Group I to the Sixth Assessment Report of the Intergovernmental Panel on Climate Change*. Cambridge University Press.

Jiang, Z., Fang, J., Mao, Y., et al., 2013. Influence of seaweed aquaculture on marine inorganic carbon dynamics and sea-air CO<sub>2</sub> flux. *J. World Aquacult. Soc.* 44 (1), 133–140.

Kormann, R., Meixner, F.X., 2001. An analytical footprint model for non-neutral stratification. *Bound.-Layer Meteorol.* 99 (2), 207–224.

Liu, S., Hu, Z., Wu, S., et al., 2016. Methane and nitrous oxide emissions reduced following conversion of rice paddies to inland crab fish aquaculture in Southeast China. *Environ. Sci. Technol.* 50 (2), 633–642.

Liu, J., Zhou, Y., Valach, A., et al., 2020. Methane emissions reduce the radiative cooling effect of a subtropical estuarine mangrove wetland by half. *Glob. Chang. Biol.* 26 (9), 4998–5016.

Lu, W., Xiao, J., Liu, F., et al., 2017. Contrasting ecosystem CO<sub>2</sub> fluxes of inland and coastal wetlands: a meta-analysis of eddy covariance data. *Glob. Chang. Biol.* 23 (3), 1180–1198.

Ma, Y., Sun, L., Liu, C., et al., 2018. A comparison of methane and nitrous oxide emissions from inland mixed-fish and crab aquaculture ponds. *Sci. Total Environ.* 637, 517–523.

Mauder, M., Cuntz, M., Drüe, C., et al., 2013. A strategy for quality and uncertainty assessment of long-term eddy-covariance measurements. *Agric. For. Meteorol.* 169, 122–135.

Morin, T.H., Bohrer, G., Naor-Azrieli, L., et al., 2014. The seasonal and diurnal dynamics of methane flux at a created urban wetland. *Ecol. Eng.* 72, 74–83.

Natchimuthu, S., Selvam, B.P., Bastviken, D., 2014. Influence of weather variables on methane and carbon dioxide flux from a shallow pond. *Biogeochemistry* 119 (1–3), 403–413.

Neubauer, S.C., Megonigal, J.P., 2015. Moving beyond global warming potentials to quantify the climatic role of ecosystems. *Ecosystems* 18 (6), 1000–1013.

Oliveira-Junior, E.S., Temmink, R.J.M., Buhler, B.F., et al., 2019. Benthivorous fish bioturbation reduces methane emissions, but increases total greenhouse gas emissions. *Freshw. Biol.* 64 (1), 197–207.

Olsson, L., Ye, S., Yu, X., et al., 2015. Factors influencing CO<sub>2</sub> and CH<sub>4</sub> emissions from coastal wetlands in the Liaohe Delta, Northeast China. *Biogeosciences* 12 (16), 4965–4977.

Qu, B., Aho, K.S., Li, C.L., et al., 2017. Greenhouse gases emissions in rivers of the Tibetan Plateau. *Sci. Rep.* 7, 8.

Raymond, P.A., Hartmann, J., Lauerwald, R., et al., 2013. Global carbon dioxide emissions from inland waters. *Nature* 503 (7476), 355–359.

Reichstein, M., Falge, E., Baldocchi, D., et al., 2005. On the separation of net ecosystem exchange into assimilation and ecosystem respiration: review and improved algorithm. *Glob. Chang. Biol.* 11 (9), 1424–1439.

Ren, W., 2021. Study on the removable carbon sink estimation and decomposition of influencing factors of mariculture shellfish and algae in China—a two-dimensional perspective based on scale and structure. *Environ. Sci. Pollut. Res.* 28 (17), 21528–21539.

Rutegwa, M., Gebauer, R., Vesely, L., et al., 2019. Diffusive methane emissions from temperate semi-intensive carp ponds. *Aquacult. Environ. Interact.* 11, 19–30.

Shaher, S., Chanda, A., Das, S., et al., 2020. Summer methane emissions from sewage water-fed tropical shallow aquaculture ponds characterized by different water depths. *Environ. Sci. Pollut. Res.* Int. 27 (15), 18182–18195.

Shiau, Y.-J., Burchell, M.R., Krauss, K.W., et al., 2016. Greenhouse gas emissions from a created brackish marsh in eastern North Carolina. *Wetlands* 36 (6), 1009–1024.

Silvennoinen, H., Liikanen, A., Rintala, J., et al., 2008. Greenhouse gas fluxes from the eutrophic temmesjoki river and its estuary in the Liminganlahti Bay (the Baltic Sea). *Biogeochemistry* 90 (2), 193–208.

- Teodoru, C.R., Nyoni, F.C., Borges, A.V., et al., 2015. Dynamics of greenhouse gases (CO<sub>2</sub>, CH<sub>4</sub>, N<sub>2</sub>O) along the Zambezi River and major tributaries, and their importance in the riverine carbon budget. *Biogeosciences* 12 (8), 2431–2453.
- Turolla, E., Castaldelli, G., Fano, E.A., et al., 2020. Life cycle assessment (LCA) proves that Manila clam farming (*ruditapes philippinarum*) is a fully sustainable aquaculture practice and a carbon sink. *Sustainability* 12 (13).
- Vallejo, B., Ponce, R., Ortega, T., et al., 2021. Greenhouse gas dynamics in a coastal lagoon during the recovery of the macrophyte meadow (Mar Menor, SE Spain). *Sci. Total Environ.* 779, 18.
- Van Dam, B.R., Lopes, C.C., Polsenaere, P., et al., 2021. Water temperature control on CO<sub>2</sub> flux and evaporation over a subtropical seagrass meadow revealed by atmospheric eddy covariance. *Limnol. Oceanogr.* 66 (2), 510–527.
- Villa, J.A., Ju, Y., Vines, C., et al., 2019. Relationships between methane and carbon dioxide fluxes in a temperate cattail-dominated freshwater wetland. *J. Geophys. Res. Biogeosci.* 124 (7), 2076–2089.
- Wilson, B.J., Mortazavi, B., Kiene, R.P., 2015. Spatial and temporal variability in carbon dioxide and methane exchange at three coastal marshes along a salinity gradient in a northern Gulf of Mexico estuary. *Biogeochemistry* 123 (3), 329–347.
- Woszczyk, M., Schubert, C.J., 2021. Greenhouse gas emissions from Baltic coastal lakes. *Sci. Total Environ.* 755, 12.
- Wu, S., Hu, Z.Q., Hu, T., et al., 2018. Annual methane and nitrous oxide emissions from rice paddies and inland fish aquaculture wetlands in Southeast China. *Atmos. Environ.* 175, 135–144.
- Xing, Y.P., Xie, P., Yang, H., et al., 2005. Methane and carbon dioxide fluxes from a shallow hypereutrophic subtropical Lake in China. *Atmos. Environ.* 39 (30), 5532–5540.
- Xiong, Y., Wang, F., Guo, X., et al., 2017. Carbon dioxide and methane fluxes across the sediment-water interface in different grass carp *Ctenopharyngodon idella* polyculture models. *Aquacult. Environ. Interact.* 9, 45–56.
- Yang, L., Lu, F., Wang, X.K., et al., 2013. Spatial and seasonal variability of diffusive methane emissions from the Three Gorges Reservoir. *J. Geophys. Res. Biogeosci.* 118 (2), 471–481.
- Yang, P., Bastviken, D., Lai, D.Y.F., et al., 2017. Effects of coastal marsh conversion to shrimp aquaculture ponds on CH<sub>4</sub> and N<sub>2</sub>O emissions. *Estuar. Coast. Shelf Sci.* 199, 125–131.
- Yang, P., Lai, D.Y.F., Huang, J.F., et al., 2018a. Effect of drainage on CO<sub>2</sub>, CH<sub>4</sub>, and N<sub>2</sub>O fluxes from aquaculture ponds during winter in a subtropical estuary of China. *J. Environ. Sci.* 65, 72–82.
- Yang, P., Zhang, Y., Lai, D.Y.F., et al., 2018b. Fluxes of carbon dioxide and methane across the water-atmosphere interface of aquaculture shrimp ponds in two subtropical estuaries: the effect of temperature, substrate, salinity and nitrate. *Sci. Total Environ.* 635, 1025–1035.
- Yang, P., Lai, D.F., Yang, H., et al., 2019a. Carbon dioxide dynamics from sediment, sediment-water interface and overlying water in the aquaculture shrimp ponds in subtropical estuaries, Southeast China. *J. Environ. Manag.* 236, 224–235.
- Yang, P., Zhang, Y., Yang, H., et al., 2019b. Large fine-scale spatiotemporal variations of CH<sub>4</sub> diffusive fluxes from shrimp aquaculture ponds affected by organic matter supply and aeration in Southeast China. *J. Geophys. Res. Biogeosci.* 124 (5), 1290–1307.
- Yang, P., Wang, D., Lai, D.Y.F., et al., 2020a. Spatial variations of N<sub>2</sub>O fluxes across the water-air interface of mariculture ponds in a subtropical estuary in Southeast China. *J. Geophys. Res. Biogeosci.* 125 (9).
- Yang, P., Zhang, Y., Yang, H., et al., 2020b. Ebullition was a major pathway of methane emissions from the aquaculture ponds in Southeast China. *Water Res.* 184.
- Yuan, J., Xiang, J., Liu, D., et al., 2019. Rapid growth in greenhouse gas emissions from the adoption of industrial-scale aquaculture. *Nat. Clim. Chang.* 9 (4), 318–322.
- Yuan, J., Liu, D., Xiang, J., et al., 2021. Methane and nitrous oxide have separated production zones and distinct emission pathways in freshwater aquaculture ponds. *Water Res.* 190, 116739.
- Zhang, M., Xiao, Q., Zhang, Z., et al., 2019. Methane flux dynamics in a submerged aquatic vegetation zone in a subtropical lake. *Sci. Total Environ.* 672, 400–409.
- Zhang, D., Tian, X., Dong, S., et al., 2020a. Carbon budgets of two typical polyculture pond systems in coastal China and their potential roles in the global carbon cycle. *Aquacult. Environ. Interact.* 12, 105–115.
- Zhang, D., Tian, X., Dong, S., et al., 2020b. Carbon dioxide fluxes from two typical mariculture polyculture systems in coastal China. *Aquaculture* 521.
- Zhao, Y., Wu, B.F., Zeng, Y., 2013. Spatial and temporal patterns of greenhouse gas emissions from Three Gorges Reservoir of China. *Biogeosciences* 10 (2), 1219–1230.
- Zhao, J., Zhang, M., Xiao, W., et al., 2019. An evaluation of the flux-gradient and the eddy covariance method to measure CH<sub>4</sub>, CO<sub>2</sub>, and H<sub>2</sub>O fluxes from small ponds. *Agric. For. Meteorol.* 275, 255–264.
- Zhu, L., Che, X., Liu, H., et al., 2016. Greenhouse gas emissions and comprehensive greenhouse effect potential of *Megalobrama amblycephala* culture pond ecosystems in a 3-month growing season. *Aquac. Int.* 24 (4), 893–902.
- Zhu, X., Qin, Z., Song, L., 2021a. How land-sea interaction of tidal and sea breeze activity affect mangrove net ecosystem exchange? *J. Geophys. Res. Atmos.* 126 (8).
- Zhu, X., Sun, C., Qin, Z., 2021b. Drought-induced salinity enhancement weakens mangrove greenhouse gas cycling. *J. Geophys. Res. Biogeosci.* 126 (8).